Joint User Association, Power Optimization and Trajectory Control in an Integrated Satellite-Aerial-Terrestrial Network

Farhan Pervez, Lian Zhao, *Senior Member, IEEE*, and Cungang Yang

***Abstract*— Internet-of-Things (IoT) is being widely embraced with the number of connected devices growing rapidly. Moreover, IoT applications are emerging in diverse verticals such as connected cars, connected factories, and smart agriculture. For new business models, in order to meet key network performance indicators, connectivity must be flexible and agile. An integrated satellite-aerial-terrestrial network (I-SAT) has recently stimulated interest in providing wireless communication due to its high maneuverability, versatile deployment, and pervasive connectivity. The resource planning, task distribution, and action management of an I-SAT can be accomplished through effective acquisition, coordination, transmission, and aggregation of diverse information. This paper considers an I-SAT network, in which multiple unmanned aerial vehicles (UAVs) with aerial stations and a terrestrial base station (BS), in a cognitive setting, in the presence of satellite-receiver communication, are deployed to support smart vehicles on the ground. By taking into account different limitations and Quality of Service (QoS) constraints, the goal is to maximize the average throughput among users by jointly optimizing user association, BS/UAV transmission power, and UAV trajectory. The formulated problem is a non-convex optimization problem with a complicated expression that is hard to solve. To tackle this problem, an alternating iterative algorithm based on the block descent method is proposed. Precisely, the problem is subdivided into three subproblems, transmitter-vehicle association optimization, BS/UAV power allocation optimization, and UAV trajectory control. Then, in an iterative process, these subproblems are solved sequentially. The proposed solution uses a segment-by-segment technique, which breaks the complete UAV flight trajectory into smaller time segments to reduce computation time when the network service period is considerable. As a result, each time segment's optimization can be solved more quickly. Furthermore, the paper presents the results of network simulations carried out to assess the efficiency of the proposed solution. The findings show that the presented scheme outperforms different benchmark schemes in terms of the average user throughput when observing multiple different scenarios.**

***Index Terms*— Integrated networks, unmanned aerial vehicles (UAVs), satellite communications, cognitive radio (CR), throughput maximization, user association, power optimization, trajectory control.**

Manuscript received April 25, 2021; revised August 10, 2021; accepted October 1, 2021. Date of publication October 21, 2021; date of current version May 10, 2022. This work was supported in part by the Natural Sciences and Engineering Research Council of Canada (NSERC) under Grant RGPIN-2020-04678. The associate editor coordinating the review of this article and approving it for publication was D. Niyato. *(Corresponding author: Lian Zhao.)*

The authors are with the Department of Electrical, Computer and Biomedical Engineering, Ryerson University, Toronto, ON M5B 2K3, Canada (e-mail: farhan.pervez@ryerson.ca; l5zhao@ryerson.ca; cungang@ryerson.ca).

Color versions of one or more figures in this article are available at https://doi.org/10.1109/TWC.2021.3120264.

Digital Object Identifier 10.1109/TWC.2021.3120264

I. Introduction

AN ENORMOUS number of people and devices can share information thanks to advancements in the interconnectivity of network artifacts using state-of-the-art communication protocols for various Internet-of-Things (IoT) applications [1]. According to a recent IoT strategies report, 30.9 billion IoT devices would be connected by 2025 delivering services such as smart cities, intelligent transport, and mission-critical assistance [2]. With the deployment of commercial 5th generation (5G) cellular networks, various segments of these services, especially in urban areas, can be effectively supported by the ground base stations (BSs) of terrestrial network through advanced system architecture and densely deployed infrastructure [3], [4]. Additionally, a satellite network that could provide services for outlying areas, is transforming into an essential medium for IoT applications such as wildlife monitoring and disaster management [5]. To provide ubiquitous service that meets end-to-end user requirements, one idea is to use a two-tier conventional satellite-terrestrial hybrid network operating in the Ka-band. However, due to scarce resources, costly maintenance, and round-trip delays, such a network is neither efficient nor cost-effective. Therefore, owing to relatively low cost and flexible movement, unmanned aerial vehicles (UAVs) based aerial communication is emerging as an enticing paradigm for IoT. Thus, the research community is discussing a triple-tier integrated satellite-aerial-terrestrial (I-SAT) network for the future 6th generation (6G) systems [6].

Although I-SAT networks provide a promising global IoT infrastructure, the ubiquitous deployment of IoT devices and systems cumulates a large volume of data into the network, resulting in spectrum scarcity. This issue cannot be resolved through traditional spectrum management approaches as they suffer the limitations of adaptability and scalability. The International Telecommunication Union Radiocommunication (ITU-R) sector has only reserved 500 MHz of Ka-band each for downlink and uplink for satellite connections, and the remainder of the Ka-band assigned to satellite communications is shared with terrestrial fixed services [7]. Moreover, for conventional aerial communications, an overcrowded unlicensed spectrum band has been used [8]. An exclusive spectrum regulation will result in an inefficient and unbalanced spectrum

use, exacerbating the problem of limited spectrum for a continuously growing IoT network. In this context, cognitive radio (CR), which uses dynamic spectrum access to solve the spectrum scarcity problem and increase spectrum efficiency, is seen as a promising solution for IoT applications [9]. Driven by the advantages of incorporating CR into satellite-terrestrial and aerial-terrestrial networks, as well as the IoT's promising future applications, we formulated and resolved a throughput maximization problem in [10], by jointly optimizing transmission power and UAV trajectory, for smart vehicles connected to the aerial-terrestrial network in a CR incorporated I-SAT environment. In this paper, we re-formulate the objective function by taking into account user association as well. The modified problem sets the connectivity and Quality of Service (QoS) constraint showing that the link established between the vehicle and transmitter affects the problem analysis.

In cognitive radio networks, there are two types of users. The first is primary users (PUs), who operate on their own licensed spectrum bands. The second is cognitive users (CUs), who can only operate on licensed spectrum bands if interference to the corresponding PUs is below a certain level. In this paper we present a novel solution for a joint user association, power optimization, and UAV trajectory control problem where the smart vehicles are CUs served by the aerial-terrestrial network operating in the Ka-band, whereas, the satellite receiver is a PU. Consequently, an I-SAT network have to make use of the CR intelligence and make sure the service requirements for both PU and CUs are satisfied. Fig. 1 shows a typical system architecture with the three network segments in an integrated satellite-aerial-terrestrial network. The terms UAV and base station are frequently interchanged in the text with aerial station and terrestrial station, respectively. The three network segments can be described as follows:

- Broadcast and multicast services are primarily provided by the satellite network segment, which includes geostationary orbit (GEO), medium earth orbit (MEO), and low earth orbit (LEO) satellites with wide coverage capabilities. Additionally, satellite networks are evolving to high throughput satellite systems in order to realise the next generation Terabit/s satellite infrastructure [11].
- The aerial network segment, which includes UAVs, unmanned airships, and balloons, can improve capacity in hotspot areas and provide timely coverage for emergency scenarios due to its lower altitude (about tens of kilometres above the earth) and versatile movement. Since a single UAV's service capability is minimal, forming a UAV swarm using multiple UAVs is critical for network's wider range.
- Ultra-densely deployed cellular cells are increasing in the terrestrial network segment amid the development of the 5G standard to enable intensive services that can be classified into three types: enhanced mobile broadband (eMBB), ultra-reliable and low-latency communications (URLLC), and massive machine-type communications (mMTC).

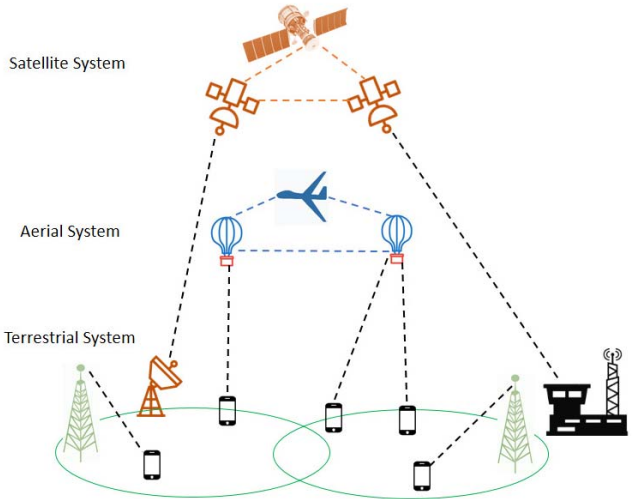

Fig. 1. System architecture of a cognitive integrated satellite-aerial-terrestrial (I-SAT) network.

Additionally, for such a multi-layer, heterogeneous, dynamic, and complex network, a software-defined network (SDN) control center is deployed to implement logically unified network management and intelligent cognition among the different network segments. This work explores the intelligent cognition part in order to maximize the average rate among all the vehicles connected to the aerial-terrestrial network in a CR-based I-SAT model by jointly optimizing the user association, UAV trajectory, and UAV/BS transmit power in a given finite period.

II. Related Research and Contribution

To cater to the insufficient spectrum issue in wireless networks, existing literature largely utilizes two-tier CR-based spectrum reusing between satellite-terrestrial or aerial-terrestrial network segments. It primarily focuses on efficient resource allocation to manage interference caused by inter-segment co-channel interference. For cognitive aerial-terrestrial networks, the authors in [12] optimized the transmission rate and power allocation of UAV to maximize the throughput of the terrestrial users. To show the impact of incorporating a UAV-based aerial station into cellular networks, the coverage probability of a cellular network that covers both aerial and terrestrial users was theoretically examined in [13]. The authors in [14] optimized the trajectory of the UAV and transmit power of both terrestrial BS and UAV to maximize the achievable rate of terrestrial users, taking interference and UAV mobility into account. In the case of a cellular network serving both UAV and terrestrial users, the UAV transmit rate and power allocation were optimized to maximize the weighted sum-rate of the UAV and terrestrial users in [15]. Considering the coexistence between the UAV and terrestrial network, UAV deployment, as well as transmission power of UAVs for a terrestrial IoT device cluster, to minimize system power consumption, were investigated in [16].

Moreover, for cognitive satellite-terrestrial networks, the authors in [17] designed a cognitive zone to guarantee the

interference threshold compliance for primary satellite communication while providing high service availability to secondary terrestrial users. In [18], the authors formulated and analyzed a power allocation strategy from the energy and spectral efficiency tradeoff perspective while guaranteeing the interference power constraint imposed by the satellite network. The authors of [19] conducted power allocation for cognitive hybrid satellite-terrestrial networks with amplify-and-forward relays in order to optimize the achievable rate. Besides, the authors in [20] performed power management for real-time satellite applications in cognitive satellite-terrestrial networks to optimize the delay-limited capacity without degrading the transmission efficiency of the primary terrestrial consumer.

However, a three-tier cognitive network has had a limited research exposure to efficiently support IoT applications. The authors in [21] explored multi-domain resource allocation for a cognitive satellite-UAV network consisting of a satellite and a swarm of UAVs, in order to increase the access efficiency in coverage gaps. The cell-free on-demand coverage, in particular, was designed to solve the cost inefficiency of traditional cellular architecture. Despite these achievements, a three-tier cognitive network nevertheless faces obstacles to efficiently support applications such as moving smart vehicles. On the one hand, implementing a dense conventional cellular architecture over a vast area to support a large number of smart vehicles is cost-ineffective. On the other hand, multi-domain resources, such as user affiliation, BS/UAV transmit power, and UAV trajectories, should be allocated jointly rather than separately to ensure that the network is centered on the desired objective. In [10], we worked on a problem that takes into consideration power and trajectory control, whereas, this work is an extension that broadens the problem and align it more with a real-time model.

In this paper, we consider a cognitive satellite-aerial-terrestrial network in which the moving vehicles on the ground are served by a single terrestrial station and a number of UAVs. Precisely, the BS and UAVs transmit data to the secondary users (smart vehicles) in the presence of a primary user, i.e. a satellite receiver, within the same spectrum. For protecting the performance of the primary network, the interference imposed on the SR from the transmit powers of the BS and UAVs has to be lower than the predefined threshold for utilizing the licensed spectrum of the satellite network, which means that the vehicle-transmitter associations, the transmission powers of the BS and the UAVs, and the UAVs trajectory, should be carefully designed in an I-SAT environment. On one side, if the BS and UAV allocate more power to transmit to smart vehicles, more interference will be imposed on the SR. On the other side, if a UAV proceeds farther away from the primary user, or moves closer to a smart vehicle, it can transmit at a higher power to enhance the cognitive network throughput. Contingent on this fact, this paper aims to maximize the smart vehicles' achievable throughput by jointly optimizing user association, BS/UAV transmit power allocations and UAVs trajectory with the user QoS provision constraints, SR interference threshold constraints and UAV mobility constraints. This challenging problem is solved by utilizing the block descent technique as used in [22], [23].

Major contributions of this paper are listed as follows:

- Firstly, to improve network efficiency, we formulate a throughput maximization problem under multiple set constraints to cater to a multi-tier CR network. However, the formulated problem is shown to be non-convex with complex expression, and there is no standard method for solving it. We break down the original problem into three subproblems in order to resolve this task, where user association, transmit powers of terrestrial base station and UAVs, and movement of UAVs are solved by using the block descent method. The original problem is solved iteratively based on the solutions to these subproblems, resulting in a low-complexity joint multi-domain optimization.
- Additionally, we implement a segment-by-segment strategy that divides the entire UAV flight trajectory into smaller time segments in order to minimize the computation time when the network service period is long. As a result, the optimization for each time segment can be solved more efficiently.
- Moreover, we evaluate the performance of the proposed solution by network simulations. The results confirm that the proposed scheme provides an improvement in terms of average user throughput compared to various standard techniques when observing multiple different scenarios.

The rest of this paper is organized as follows. Section III and Section IV introduce the system model and the problem formulation for an integrated terrestrial and non-terrestrial network, respectively. In Section V, we propose an efficient iterative algorithm to solve the formulated problem by applying the subproblem technique. Section VI presents the numerical results to demonstrate the performance of the proposed design. Finally, we conclude the paper in Section VII.

III. System Model

We consider an UAV-enabled terrestrial network as shown in the schematic diagram given in Fig. 2, where multiple UAVs and a BS serve as transmitters to provide network connectivity to K number of vehicles. The transmitters and the terminals at smart vehicles are both equipped with a single antenna each. Let k be the index of user terminals, $k \in \{1, 2, ..., K\}$, and let q be the index of UAVs, $q \in \{1, 2, ..., Q\}$. Moreover, the UAV-aided terrestrial network shares the same spectrum with the satellite network, where the satellite connects with the satellite receiver on the ground while the BS/UAVs transmit data to the terrestrial vehicles. As highlighted in Fig. 2, we can see that a UAV q serves its associated users over different channels. Additionally, the UAV can cause interference to other non-associated vehicles and the satellite receiver. Besides, the UAVs can freely adjust their horizontal plane trajectory while keeping a fixed altitude, H_u, within a time horizon of C seconds. The horizontal coordinate of the satellite receiver r, terrestrial vehicle k, and BS b are respectively denoted as w_r, w_k, and w_b. In addition, the altitude of BS, which is the antenna height from ground, is fixed with H_b. The model also shows that the aerial stations are wirelessly connected with the network through free space optical (FSO)

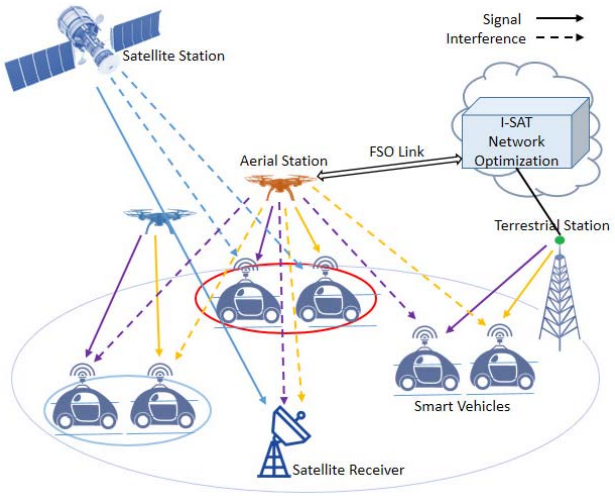

Fig. 2. Schematic diagram of the considered integrated model.

links [24]. Whereas, the optimization for the whole model in line with the objective function can be performed in the network cloud. Here, in order to have a more tractable problem, the time horizon is equally divided into T time slots, $t \in \{1, 2, ..., T\}$, with each slot duration $\delta = C/T$. Therefore, the horizontal coordinates of UAV q at time slot t can be denoted as $f_q[t]$, $\forall t$. Moreover, because of its high mobility and stationary properties, we consider a rotary-wing UAV [25].

A. BS-Terrestrial User Channel Model

Assuming Rayleigh fading occurs between the BS and the smart vehicle (SV) or satellite receiver (SR), the channel power gain between the BS, b, and the SR, r, at time interval t, can be represented as [26]:

$$g_{rb}[t] = \frac{\beta_o}{(H_b^2 + \|w_b - w_r\|^2)^{\frac{\alpha}{2}}} \upsilon_r, \tag{1}$$

where β_o is the reference channel gain at distance 1m, α denotes path-loss exponent, and υ_r is an independent and identically distributed (i.i.d.) exponential random variable with unit mean accounting for the small-scale Rayleigh fading.

Whereas, the channel power gain between the BS and SV k can be given as:

$$h_{kb}[t] = \frac{\beta_o}{(H_b^2 + \|w_b - w_k\|^2)^{\frac{\alpha}{2}}} \upsilon_k. \tag{2}$$

where υ_k is also an i.i.d. exponential random variable with unit mean accounting for the small-scale Rayleigh fading.

B. UAV-Terrestrial User Channel Model

A widely used air-to-ground (A2G) free-space path loss model is used for ease of analysis [27]. Since the UAV travels at a high altitude and the line-of-sight (LoS) is dominated, the free-space path loss model does not account for small-scale fast fading. Moreover, the Doppler effect caused by the UAV's mobility is considered to be perfectly compensated at the SV/SR [28]. Hence, the channel gain from UAV q to SR r at time slot t can be given as:

$$g_{rq}[t] = \frac{\beta_o}{H_u^2 + \|f_q[t] - w_r\|^2}, \tag{3}$$

whereas, the channel gain from UAV to SV k at time slot t can be given as:

$$h_{kq}[t] = \frac{\beta_o}{H_u^2 + \|f_q[t] - w_k\|^2}. \tag{4}$$

C. Satellite-Terrestrial User Channel Model

Similar to our assumptions for aerial-terrestrial channel model, the satellite-terrestrial link between the satellite and SV also considers a LoS environment. Moreover, due to very high altitudes, it is assumed to be invariant over time slots [29]. Therefore, the channel gain from satellite s to SV k can be expressed as:

$$h_{ks} = \frac{\beta_o}{D^2 + \|w_s - w_k\|^2}, \tag{5}$$

where D gives satellite altitude above the ground and w_s are the satellite horizontal coordinates.

The transmit power of the satellite is denoted as P_{SS}, and it is assumed to be invariant over time slots. Moreover, we express the total number of transmitters as M, such that $m \in \{1, 2, ..., M\}$, including Q UAVs and one BS. The vehicles can connect to any of the transmitters that provide the best channel state information (CSI) over the downlink. The fast fading is averaged out, and perfect CSI is considered, as user association occurs over a large time scale relative to channel transition. Let n be the index of channels available, $n \in \{1, 2, ..., N\}$. There are a total of N channels available for each transmitter, however, a vehicle is assigned one channel only.

Therefore, the achievable rate for vehicle k connected to transmitter m over channel n at time t is given as:

$$R_{kmn}[t] = B_m \cdot \log_2 \left(1 + \gamma_{kmn}[t]\right), \tag{6}$$

where B_m denotes the channel bandwidth and γ_{kmn} gives the signal-to-interference-plus-noise ratio (SINR) for vehicle k that can be expressed as:

$$\gamma_{kmn}[t] = \frac{p_{mn}[t] h_{km}[t]}{\sum_{j \neq m} p_{jn}[t] h_{kj}[t] + P_{SS} h_{ks} + \sigma_k^2}, \tag{7}$$

where p_{mn} gives the transmit power for a transmitter m over channel n, h_{km} represents the channel gain from the transmitter to SV. Besides, unit directional antenna gain is considered. Moreover, h_{ks} is the channel gain from satellite to SV. Whereas, σ_k^2 gives the power of additive white Gaussian noise (AWGN) at SV.

In addition, the received interference from the BS and UAVs to the SR r within time slot t is given as,

$$\zeta^r[t] = \sum_m \sum_n p_{mn}[t] g_{rm}[t], \tag{8}$$

where g_{rm} gives the channel gain from transmitter m to the satellite receiver.

We can see from the above expressions that both the BS/UAV transmit power and the UAV trajectory have a major effect not only on the SVs achievable rate but also on the SR interference. Increased BS/UAV transmit power, in particular, would boost the SV achievable rate while increasing SR interference. Additionally, as the UAV approaches SR, the obtained interference at SR will increase. Since the SV and the SR share the same spectrum, the power allocated for transmission from BS/UAVs should be restricted so that the BS/UAVs network's interference with the SR is less than the interference threshold value [18]. Hence, we have to carefully design the I-SAT network.

IV. Problem Formulation

Over a given horizon time C, our goal is to maximize the total achievable rate of all connected vehicles K by jointly optimizing vehicle association, BS/UAV power allocation as well as UAV trajectory. Accordingly, the problem can be formulated as follows:

$$\min_{\boldsymbol{\mu},\mathbf{p},\mathbf{f}} \sum_t \sum_k \sum_m \sum_n \mu_{kmn}[t] R_{kmn}[t], \tag{9a}$$

$$\text{s.t} \sum_k \mu_{kmn}[t] \leq A_m, \quad \forall m, n \tag{9b}$$

$$\sum_m \sum_n \mu_{kmn}[t] = 1, \quad \forall k, \tag{9c}$$

$$\mu_{kmn}[t] \in \{0,1\}, \quad \forall k, m, n \tag{9d}$$

$$\gamma_{kmn}[t] \geq \gamma_k^{min}, \quad \forall k \tag{9e}$$

$$\zeta^r[t] \leq \zeta_{th}, \quad \forall t \tag{9f}$$

$$0 \leq p_{mn}[t] \leq p_m^{max}, \quad \forall m, n \tag{9g}$$

$$f_q[1] = f_q[T], \quad \forall q, \tag{9h}$$

$$\|f_q[t+1] - f_q[t]\|^2 \leq V_q^{max}\delta, \quad t = 1, \ldots, T-1, \tag{9i}$$

$$\|f_q[t] - f_i[t]\|^2 \geq \chi_{min}^2, \quad \forall t, i, i \neq q, \tag{9j}$$

where the constraint in (9b) refers to maximum number of users a transmitter can serve, and (9c), and (9d) indicate that at any point in time, one vehicle may only be paired with one transmitter. The binary variable $\mu = \mu_{kmn}$ serves as the association indicator for channel assignment and transmitter association for each ground user (i.e., $\mu_{kmn} = 1$ means user k is served by transmitter m on channel n while $\mu_{kmn} = 0$ means otherwise). This set of constraints guarantees that each ground user is served uniformly by one resource block (i.e., by a single transmitter on a single channel at a time) and that each resource block can only support one ground user at a time. The constraint in (9e) specifies that the user's received downlink SINR cannot be less than the minimum SINR requirement in order to fulfill QoS provision for end users. Constraint (9f) denotes the maximum interference threshold (IT) the satellite receiver can tolerate, whereas, (9g) gives the minimum and maximum transmission power limits for the UAVs and BS. Constraint (9h) expresses that the UAV returns to its initial location at the end of time horizon C. Moreover, UAV trajectories are also dependent upon the maximum speed as given in (9i) and the collision avoidance as given in (9j). The V_q^{max} in (9i) expresses the maximum speed in meters/second (m/s), whereas, χ_{min} in (9j) gives the minimum distance in meters between two UAVs to ensure collision avoidance. By choosing a sufficiently small time slot, δ, UAV's location is assumed to be unchanged within each interval.

V. Proposed Solution

In this section, we focus on the solution of the objective function presented in Section IV. The problem can be split into three subproblems: user association, transmission power optimization, and UAV trajectory control, all of which are alternately solved in order to increase the downlink average throughput of the vehicles connected to the network. The three subproblems are investigated separately in the following parts. Finally, a joint algorithm is proposed by integrating all three subproblems in the last part.

A. User Association Optimization

Given transmission power allocation and location of the transmitters, and taking into consideration that maximizing for every interval, t, leads to maximizing rate over time horizon C, we formulate an user association optimization sub-problem. The sub-problem considers assigning only one channel for each vehicle, k, and involves finding the indicators μ_{km} corresponding to the association (i.e., $\mu_{km} = 1$ when user k is associated with transmitter m, $\mu_{km} = 0$ otherwise), that can maximize the overall utility for all the vehicles connected. The vehicle-transmitter association is assumed to be carried out on a larger time interval compared to the change of channel, therefore, the SINR is averaged over the association time. Here, we suppose that the transmission power is equally distributed among all sub-carriers. Hence, we can write the relaxed version of the user association optimization problem as:

$$\max_{\boldsymbol{\mu}} \sum_k \sum_m \mu_{km} R_{km}, \tag{10a}$$

$$\text{s.t} \sum_k \mu_{km} \leq A_m, \quad \forall m \tag{10b}$$

$$\sum_m \mu_{km} = 1, \quad \forall k, \tag{10c}$$

$$\mu_{km} \in \{0,1\}, \quad \forall k, m \tag{10d}$$

$$\sum_m \mu_{km} \gamma_{km} \geq \gamma_k^{min}, \quad \forall k \tag{10e}$$

where A_m in (10b) is introduced as a load metric denoting the maximum number of associations a transmitter m can have with vehicles in the system. (10c) and (10d) imply that one user can be associated with one transmitter, whereas, (10e) deals with the QoS requirements.

We build an algorithm using the Lagrangian multiplier method in order to effectively solve this problem [30], [31]. Here, a low-complexity distributed user association algorithm is proposed based on the Lagrangian dual analysis to ensure the defined goal is met under the given constraints. Furthermore, the algorithm has been shown to converge to the dual problem's global optimum. In order to determine an optimal

solution to the subproblem, the Lagrangian function can be expressed as below:

$$\begin{aligned} &L(\boldsymbol{\mu}, \mathbf{A,\ c,\ d}) \\ &= \sum_k \sum_m \mu_{km} R_{km} - \sum_m A_m \log(A_m) \\ &\quad - \sum_m c_m (\sum_k \mu_{km} - A_m) - \sum_k d_k (\gamma_k^{min} - \sum_m \mu_{km} \gamma_{km}), \end{aligned} \tag{11}$$

where c_m and d_k are both nonnegative Lagrange multipliers. Consequently, the dual function $\Omega(\cdot)$ can be given as

$$\min_{\mathbf{c,d}} \Omega(\mathbf{c,\ d}) = \begin{cases} \max_{\boldsymbol{\mu}, \mathbf{A}} L(\boldsymbol{\mu}, \mathbf{A,\ c,\ d}) \\ s.t. \\ \sum_m \mu_{km} = 1, \quad \forall k \\ \mu_{km} \in \{0, 1\}, \quad \forall k, m \\ \mathbf{c,\ d} \geq 0. \end{cases} \tag{12}$$

The analytic solution to the Lagrangian maximization is as follows:

$$\mu_{km}^* = \begin{cases} 1, & \text{if } m = m^* \\ 0, & \text{if } m \neq m^*, \end{cases} \tag{13}$$

where

$$m^* = arg \max_m \left(R_{km} - c_m + d_k \gamma_{km} \right). \tag{14}$$

Setting $\partial L / \partial A_m = 0$, A_m^* can be derived as

$$A_m^* = \exp^{c_m - 1}. \tag{15}$$

For the optimal solution, we cannot get the closed form expression directly because the dual function $\Omega(\mathbf{c,\ d})$ is not a differentiable function. As a result, we introduce m^* and A_m^*, in (13) and (15), and use a subgradient method to update $\mathbf{c}$ and $\mathbf{d}$ as

$$c_m(l+1) = c_m(l) - \Delta(l) \left(A_m(l) - \sum_k \mu_{km}(l) \right), \quad \forall m, \tag{16}$$

$$d_k(l+1) = d_k(l) - \Delta(l) \left(\sum_m \mu_{km}(l)\ \gamma_{km} - \gamma_k^{min} \right), \forall k, \tag{17}$$

where the time index l indicates c and d need to be updated iteratively, and $\Delta(l)$ is the step size.

Updated $c_m(l)$ and $d_k(l)$ are used to obtain updated $\mu_{km}(l)$ and $A_m(l)$ via (13) and (15), respectively. Due to the fact that the dual problem is always convex, the sub gradient method will converge to the global optimum of (12).

Interpreting the dual variable "d" as users' dissatisfactory factor: When the received SINR for user k, $\sum_m \mu_{km} \gamma_{km}$, is higher than the minimum required SINR, γ_k^{min}, d_k will decrease. As a result, the weight of SINR value when selecting the serving transmitter through (14) will be reduced.

Interpreting the dual variable "c" as the inter-price between users and transmitters: We may deduce that $\sum_k \mu_{km}$ represents the amount of service required by users, while A_m represents the amount of service provided by the transmitter m. Therefore, when the service demand $\sum_k \mu_{km}$ is larger than the service supply A_m of transmitter m, the price c_m will increase, otherwise will decrease. Therefore, according to (14), if m is overloaded, c_m will go up, and fewer users will be associated with it.

Algorithm 1 Algorithm for User Association at Vehicle

1: **if** $l = 0$, **then**
2: Initialize $d_k(l+1)$.
3: **else**
4: Update $d_k(l+1)$ according to (17).
5: **end if**
6: $l \leftarrow l + 1$.
7: Each user measures SINR via pilot signal from all transmitters, and receives the values of $c_m(l)$, $\forall m$ via transmitter broadcast.
8: User k determines the serving transmitter m according to $m^*(l) = arg \max_m (R_{km} - c_m(l) + d_k(l)\ \gamma_{km})$.
9: Each user feedbacks the user association request to the chosen transmitter.

Algorithm 2 Algorithm for User Association at Transmitter

1: **if** $l = 0$, **then**
2: Initialize $c_m(l+1)$.
3: **else**
4: Each transmitter calculates the value of $A_m(l)$ using (15).
5: Receives the updated user association matrix $\mu_{km}(l)$ from the users.
6: Updates $c_m(l+1)$ according to (16).
7: **end if**
8: $l \leftarrow l + 1$.
9: Broadcasts the value of $c_m(l)$.

Derived from the analysis, we propose a distributed user association algorithm, which includes algorithms for the user and the transmitter ends, as seen in Algorithm 1 and Algorithm 2, respectively. Both sides execute their algorithm iteratively until convergence. The distributed algorithm has $\mathcal{O}(|M||K|)$ complexity in each iteration. In terms of data exchanged, each transmitter broadcasts c_m in each iteration, and each user only communicates its affiliation request to the chosen transmitter. Hence, the exchanged information in the proposed distributed algorithm is $(|M| + |K|)$ for each iteration. The simulation analysis verifies that when the step size is set as $\Delta(l) = 1/l$, where l is the number of iteration, the distributed algorithm converges fairly quickly with less than thirty iterations.

B. Transmit Power Optimization

Given the user association and the location of transmitters, and considering that maximizing for every interval, t, leads to maximizing the rate over time horizon C, the transmission power in problem (9a) can be optimized by solving the

following sub-problem:

$$\max_{\mathbf{p}} \sum_{m}\sum_{n} \mu_{mn} R_{mn}, \tag{18a}$$

$$\text{s.t } \zeta^r \leq \zeta_{th}, \quad \forall t \tag{18b}$$

$$0 \leq p_{mn} \leq p_m^{max}, \quad \forall m, n \tag{18c}$$

where constraint (18b) is the interference tolerance requirement at SR. Moreover, the sub-problem (18a) is strictly quasi-concave for the given constraints since the objective function (18a) is strictly concave. Hence, any local maximum is a global maximum, and (18a) has at most one maximum due to being strictly quasi-concave.

The solution of (18a) is achieved by dividing the problem into two sub-layers. The first layer performs the power allocation on the transmitter level, whereas, the second provides power distribution among different channels of each transmitter. To solve the two sub-layers, we apply a straightforward and sophisticated geometric water-filling (GWF) method given in [32] and [33]. Contrary to the conventional water-filling (CWF) technique, it eliminates the need for resolving a nonlinear system from the Karush-Kuhn-Tucker (KKT) conditions of the target problem for finding the water level. The GWF, in comparison to the CWF algorithm, requires minimal computation, with similar memory requirement and sorted parameters. Moreover, it avoids complicated derivations, such as derivative or gradient operations in conventional optimization techniques.

The first layer, that allocates power at the transmitter level and provides optimum power allocation in order to improve the efficiency of wireless transmission for all transmitters, in problem (18a), can be given as

$$\max_{\mathbf{s}} \sum_{m} \log_2\left(1 + \overline{a_m} s_m\right), \tag{19a}$$

$$\text{s.t } \sum_{m} s_m g_{rm} \leq \zeta_{th}, \tag{19b}$$

$$0 \leq s_m \leq s_m^{max}, \quad \forall m \tag{19c}$$

where $\overline{a_m}$ is the mean channel gain of N_m users connected to transmitter m and is given as

$$\overline{a_m} = \frac{1}{N_m} \cdot \sum_{k} h_{km}, \quad \forall m. \tag{20}$$

An illustration of the GWF algorithm is given in Figs. 3(a)-(b). We assume 4 steps/transmitters ($M = 4$) with unit width inside a water tank. As the number of steps in the GWF solution is the same as the number of transmitters in our system, we used M to denote the number of steps in the following analysis. The sequence $\overline{a_m}$ is sorted as monotonically decreasing, therefore, the step depth of the stairs indexed as $\{1, ..., M\}$ is monotonically increasing. When using the conventional method, firstly, the water level, ξ, needs to be figured out and then the power assigned for each stair, i.e. the water volume above the stair, is obtained. Whereas, the GWF technique, instead of trying to determine ξ, a real non-negative number, aims to determine the water level step, i.e. an integer number from 1 to M. This number, denoted by m^*, is the highest step under water. Derived from the result of m^*, we can directly write out the solution for power allocation.

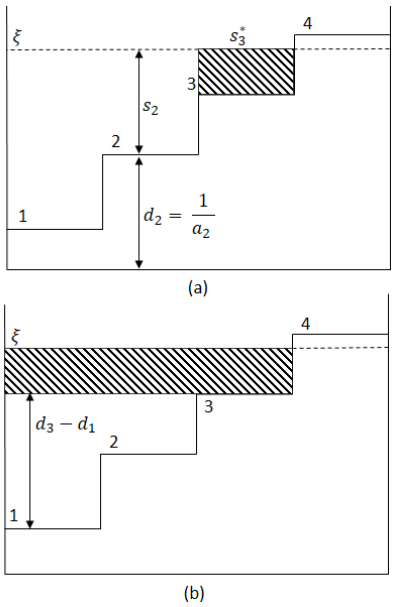

Fig. 3. Illustration for the GWF algorithm. (a) Illustration of water level step $m^* = 3$, allocated power for the third step s_3^*, and step/stair depth $d_m = 1/\overline{a_m}$. (b) Illustration of $P_A(m)$ (shadowed area, representing the total water/power above step m) when $m = 3$.

Let $P_A(m_z)$ give the water volume above step m_z for $z = \{1, ..., |E|\}$, where E is a subsequence of the sequence $\{1, ..., M\}$, $|E|$ is the cardinality of the set E, so E can be expressed as $\{m_1, m_2, ..., m_{|E|}\}$. The value of $P_A(m_z)$ can be solved by subtracting the volume of the water under step m_z from the interference threshold ζ_{th}, as

$$P_A(m_z) = \left[\zeta_{th} - \sum_{y=1}^{|E|-1} \left(d_{m_z} - d_{m_y}\right)\right]^+, \quad 1 \leq z \leq |E|, \tag{21}$$

where the step depth d_{m_z}, given by $\frac{1}{\overline{a_{m_z}}}$, is the height of the $m_z th$ step to the bottom of the water tank.

Hence, the explicit solution to (19a) is:

$$s_m = \begin{cases} \dfrac{1}{g_{rm}} \cdot \left[s_{z^*} + \left(d_{z^*} - d_m\right)\right], & 1 \leq m \leq z^* \\ 0, & z^* < m \leq M, \end{cases} \tag{22}$$

where

$$z^* = max\left\{z \mid P_A(m_z) > 0, \ \ 1 \leq z \leq |E|\right\} \tag{23}$$

and the power level for this step is

$$s_{z^*} = \frac{1}{z^*} \cdot P_A(m_{z^*}). \tag{24}$$

Algorithm 3 gives the GWF-based dynamic power distribution process at the transmitter level. The difference between the individual peak power sequence and the current power distribution sequence gives the state of this process. The process control is based on the state mentioned above and

Algorithm 3 Power Allocation at Transmitter Level

1: Input: vector d_m, s_m^{max} for $m = 1, 2, ..., M$, the set $E = 1, 2, ..., M$, and ζ_{th}.
2: Utilize (22)-(24) to compute s_m.
3: $\Lambda \Rightarrow \{m \mid s_m > s_m^{max}, m \in E\}$. If Λ is null output will be $\{s_m\}_{m=1}^{M}$ else $s_m = s_m^{max}$.
4: Update E with $E \setminus \Lambda$, update ζ_{th} with $\zeta_{th} - \sum_{x \in \Lambda} s_x$. Then return to 2:.

determined by using (22)-(24). Hence, a new state appears for the next time stage, and an optimal power allocation process with the state feedback is formed. As the finite set E reduces until the set Λ is empty, the algorithm carries out M loops to compute the optimal solution, at most.

Moreover, the second layer, that allocates power to every channel n of each transmitter, can be solved by the below given sub-problem for transmitter m:

$$\max_{\mathbf{p}} \sum_{n} \log_2 (1 + a_n p_n), \tag{25a}$$

$$\text{s.t} \sum_{n} p_n = s_m, \tag{25b}$$

$$p_n > 0, \quad \forall n \tag{25c}$$

where

$$a_n = \frac{h_{kn}}{\sum_{j \neq m} p_{jn} h_{kj} + G(\theta_{ks}) P_{SS} h_{ks} + \sigma_k^2}. \tag{26}$$

The first term in the denominator can be ignored by utilizing local partial zero-forcing precoding [34], whereas, the step depth is given as $d_n = 1/a_n$. Hence, from the explanation provided in Fig. 3, it is easy to interpret that explicit solution to (25a) is:

$$p_n = \begin{cases} p_{z^*} + (d_{z^*} - d_n), & 1 \leq n \leq z^* \\ 0, & z^* < n \leq N, \end{cases} \tag{27}$$

where z^* and the power level for this step, p_{z^*}, can be obtained by using expressions in (23) and (24), respectively. Whereas, the value of $P_A(z)$ can be solved by subtracting the volume of water under step z from the total transmitter power s_m, as

$$P_A(z) = \left[s_m - \sum_{n=1}^{z-1} (d_z - d_n) \right]^+, \quad 1 \leq z \leq N. \tag{28}$$

From the given explicit solution, we can see that when z^* is obtained, $P_A(z^*)$ is given. It is then memorized and multiplied by a constant to compute p_{z^*}. Therefore, the key point for the proposed GWF algorithm is how to search z^*, and the procedure for it is given in Algorithm 4.

C. UAV Trajectory Control

The UAV trajectory in problem (9a) can be optimized for any given user association as well as transmit powers by solving the following sub-problem:

Algorithm 4 Water-Level Step Search for Channel Power Allocation of Transmitter "m"

1: Initialize $s_m^X = s_{m^*} = s_m$; $n = 1$.
2: Compute $s_{m^*} \leq s_{m^*} - (d_{n+1} - d_n)$. Then $n \leq n + 1$, where "$\leq$" expresses the assignment operation.
3: If $s_{m^*} > 0$ and $n \leq N$, $s_m^X = s_{m^*}$, and repeat step 2); else, output $z^* = n - 1$ and $p_{z^*} = s_m^X$.

$$\max_{\mathbf{f}} \sum_{t} \sum_{q} R_q[t], \tag{29a}$$

$$\text{s.t } f_q[1] = f_q[T], \quad \forall q, \tag{29b}$$

$$\|f_q[t+1] - f_q[t]\|^2 \leq V_q^{max} \delta, \quad t = 1, \ldots, T-1, \tag{29c}$$

$$\|f_q[t] - f_i[t]\|^2 \geq \chi_{min}^2, \quad \forall t, i, i \neq q. \tag{29d}$$

where $R_q[t] = \sum_k \mu_{kq} R_{kq}$ establishes that the rate achieved by a UAV is dependent on associated users.

The non-convex constraint in (29d) means that (29a) is not concave nor quasi-concave. Therefore, to tackle the non-convexity, Lemma 1 is introduced to transform it, and an iteration-based successive convex approximation technique is used, where the original function is approximated by a more tractable function at a given local point in each iteration [22].

Lemma 1: We define a quadratic function as follows:

$$g(x) = x^2. \tag{30}$$

With a given local point x^η, at iteration η, following inequality can be given:

$$x^2 \geq 2x^\eta \times (x - x^\eta) + (x^\eta)^2. \tag{31}$$

Proof: We can observe from (30) that $g(x)$ is a convex function. Since the lower bound of any convex function can be approximated by first-order Taylor approximation at a local point, the inequality holds in (31).

We denote UAV trajectory in the ηth iteration as $F^\eta = \{f_q^\eta[t], \forall q, t\}$. For constraint (29d), since $\|f_q[t] - f_i[t]\|^2$, with respect to $f_q[t]$, is a convex function, we have the subsequent inequality based on Lemma 1:

$$\|f_q[t] - f_i[t]\|^2 \geq -\|f_q^\eta[t] - f_i^\eta[t]\|^2 + 2(f_q^\eta[t] - f_i^\eta[t])^\perp \times (f_q[t] - f_i[t]), \quad \forall i \neq q, t. \tag{32}$$

where $\perp$ gives the matrix transpose. Recalling the first-order Taylor expansion, with any given local point F^η along with the lower bound in (32), the problem can be approximated as

$$\max_{\mathbf{F}} \sum_{t} \sum_{q} R_q^\eta[t], \tag{33a}$$

$$\text{s.t } f_q[1] = f_q[T], \quad \forall q, \tag{33b}$$

$$\|f_q[t+1] - f_q[t]\|^2 \leq V_q^{max} \delta, \quad t = 1, \ldots, T-1, \tag{33c}$$

$$\chi_{min}^2 \leq -\|f_q^\eta[t] - f_i^\eta[t]\|^2 + 2(f_q^\eta[t] - f_i^\eta[t])^\perp \times (f_q[t] - f_i[t]), \quad \forall t, i, i \neq q, \tag{33d}$$

where constraint (33c) is convex quadratic and constraints (33b) and (33d) are both linear. Thus, being a convex

Algorithm 5 Alternating Algorithm for Joint Optimization

1: Initialize the BS power allocation and UAVs' power allocation and locations;
2: **while** Improvement of the downlink sum rate is higher than a predefined tolerance **do**
3: Optimize user association with fixed UAV placement and BS/UAV power allocation following Algorithm 1 and Algorithm 2;
4: Optimize BS/UAV power allocation with fixed user association and UAV placement using Algorithm 3 and Algorithm 4;
5: Optimize UAV trajectory with fixed user association and BS/UAV power allocation via standard convex optimization;
6: **end while**;
7: Output the user association indicators, UAVs' optimized location, and the BS and UAVs' downlink power allocation as the optimal solution to (9a).

optimization problem, (33a) can be effectively solved using standard convex optimization solvers such as [35]. Hence, the optimal objective value attained from (33a) serves as a lower bound of (29a) in general.

D. Alternating Optimization Algorithm

Considering the solutions presented for the three subproblems, we propose an iterative algorithm for problem (9a) by using the block descent method, also known as the alternating optimization method. The optimization variables, $\{\boldsymbol{\mu}, \mathbf{p}, \mathbf{f}\}$, in the original problem are partitioned into three blocks. Then, user association $\boldsymbol{\mu}$, transmit power $\mathbf{p}$, and UAV trajectory $\mathbf{f}$ are alternately optimized, by solving problems (10a), (18a) and (29a) sequentially, while keeping the other two blocks of variable fixed. In addition, the obtained solution in each iteration is used as the input of the next iteration. The framework is summarized in Algorithm 5.

Here, we analyze the computational complexity of our proposed algorithm. As discussed in Section IV-A, the complexity of solving (10a) is denoted by $\mathcal{O}(L(|M||K|))$, where L represents the number of iterations required for the distributed user association algorithm to converge. Similarly, the complexity of solving (18a), in Section IV-B, is denoted as $\mathcal{O}(|M| + |M||N|)$. In Section IV-C, problem (29a) is approximated as a convex one, and thus, it can be directly solved through the interior point method with complexity $\mathcal{O}(H(2Q)^3)$, where H represents the number of iterations performed by the solver. Hence, the total computational complexity of Algorithm 5 per time interval can be denoted by $\mathcal{O}(L(|M||K|) + |M| + |M||N| + H(2Q)^3)$.

VI. Numerical Results and Evaluation

In this section we present and investigate simulation results to demonstrate the efficacy of the proposed algorithm. We consider a 2000 m $\times$ 2000 m area grid for which a BS at location (0, 0), and three UAVs, starting at random locations, provide wireless connectivity for smart vehicles. Besides, we assume a unit bandwidth, whereas, other system parameters used to simulate the environment are summarized in Table I.

TABLE I
Simulation Environment

System frequency	30 GHz
AWGN power σ_k^2	-169 dBm/Hz
BS antenna height H_b	25 m
UAV height H_u	100 m
Max UAV speed V_q^{max}	30 m/s
Min inter-UAV distance χ_{min}	1 m
Max transmission power p_m^{max}	100 W
Satellite receiver IT ζ_{th}	400 W
Number of Vehicles K	60
Vehicle Speed	60 kmph
Time horizon C	100 s
Slot duration δ	1 s
Time intervals T	100

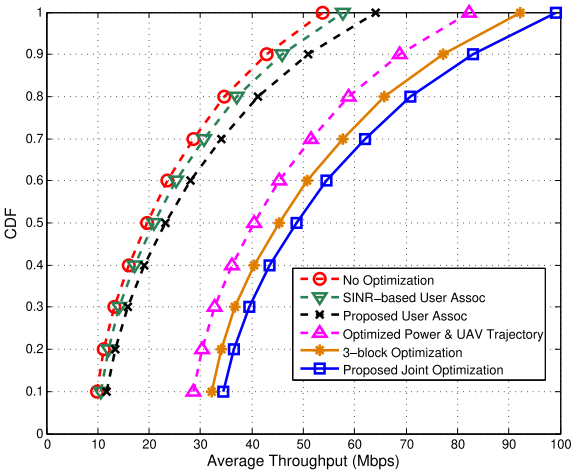

Fig. 4. CDF for the average throughput of vehicles for ten different scenarios.

To analyze our proposed joint optimization, we compare it with five different benchmark schemes. Moreover, to confirm the advantage of the proposed scheme, we investigate multiple scenarios, varying the vehicles' movement and initial locations of UAVs. The comparison between different schemes is given in Fig. 4 that shows the cumulative distribution function (CDF) for average user throughput for ten different scenarios. As shown in the figure, the "No Optimization" scheme refers to the one in which user is associated with the nearest transmitter, UAV positions are fixed, and no power optimization is performed. The "SINR-based User Assoc" scheme refers to the one in which only user association is optimized taking into account the received maximum SINR. The "Proposed User Assoc" scheme refers to the one in which only the user association is optimized using the subproblem defined in Section V-A. The "Optimized Power & UAV Trajectory" scheme is the one in which UAV positions and transmission power optimization is performed as in [10]. Whereas, "3-block Optimization" refers to the optimization proposed in [36].

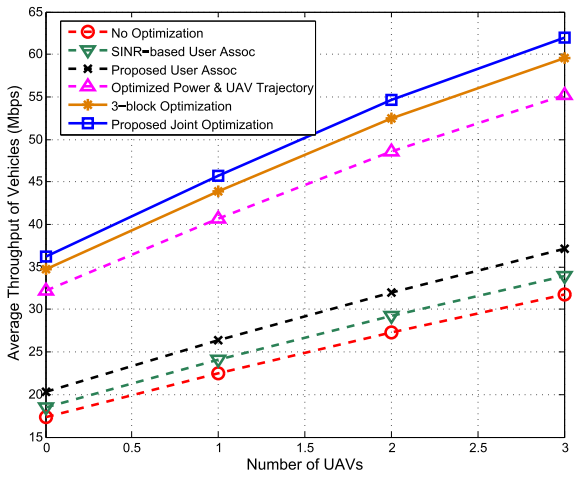

Fig. 5. Average throughput w.r.t. the number of UAVs integrated in the system.

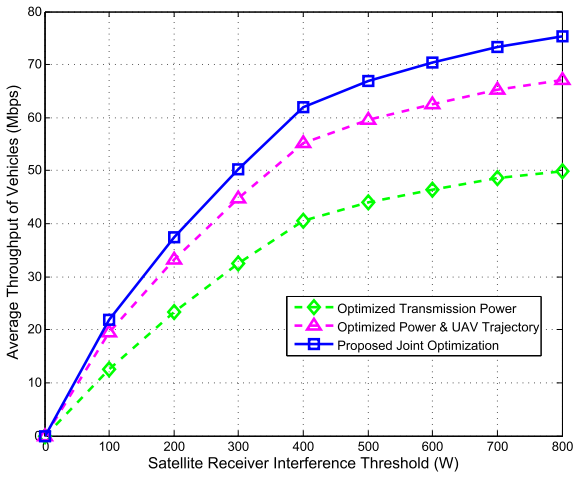

Fig. 7. Average throughput w.r.t. satellite receiver interference threshold.

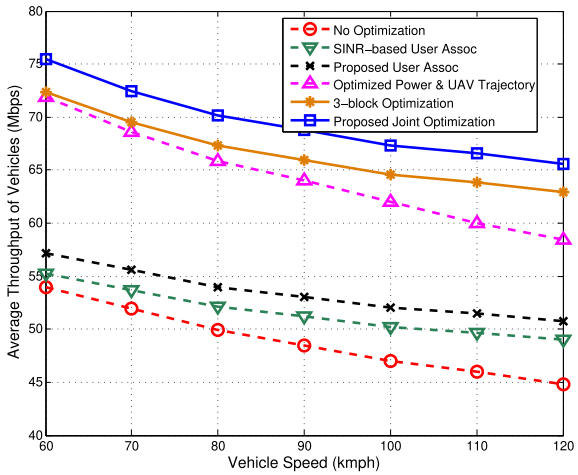

Fig. 6. Average throughput w.r.t. the vehicles speed.

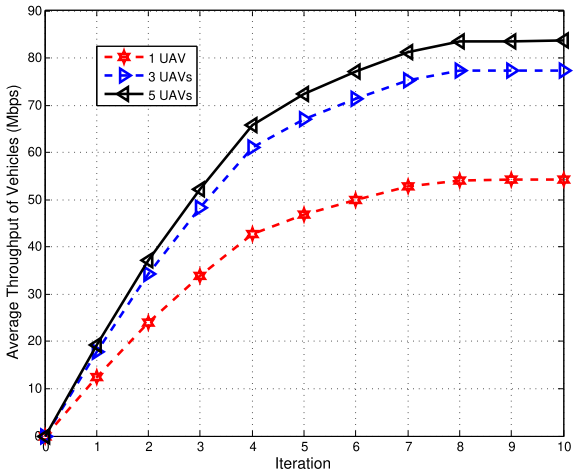

Fig. 8. Convergence of the proposed joint optimization.

It can be observed that our proposed joint optimization scheme performs much better compared to the benchmark schemes, verifying the superiority of the proposed solution.

In Fig. 5, we demonstrate the advantage of having an aerial-terrestrial network in order to serve smart vehicles. It shows that integrating UAVs within the network helps in enhancing the average user throughput. Besides, the blue curve, representing our proposed joint solution, easily outperforms all the five benchmark schemes. Moreover, Fig. 6 shows that the proposed algorithm also substantially outperforms other benchmark schemes across the simulated vehicle speed range.

Subsequently, as seen in Fig. 7, we analyze the change in average throughput by varying the satellite receiver interference threshold, ζ_{th}, setting $M = 4$ (1 BS, 3 UAVs). The comparison done is between our proposed joint optimization, "Optimized Power & UAV Trajectory" scheme, and a framework where only transmission power of BS and UAVs is optimized, referred as "Optimized Transmission Power". It is clearly seen that the proposed algorithm outperforms both benchmarks. Finally, the overall convergence performance of the proposed iterative algorithm for solving the throughput maximization problem is shown in Fig. 8. Three different scenarios are simulated, where 60 vehicles are served by one terrestrial base station and 1, 3 and 5 UAVs, respectively. Each iteration involves the optimization of user association, transmission power, and UAV trajectory. We can observe from the figure that the system throughput converges after eight iterations. Afterwards, further updating the user association, UAV locations and power allocation does not improve the throughput higher than a predefined tolerance.

VII. Conclusion

The Internet of Things (IoT) is gaining popularity, and the number of linked devices is fast increasing. In addition, IoT applications are gaining traction in a variety of industries, including connected vehicles. Connectivity must be flexible and adaptable to support new business models and achieve critical network performance parameters. Due to its high mobility, variable deployment, and pervasive connectivity, an integrated satellite-aerial-terrestrial (I-SAT) network has lately sparked interest in providing efficient wireless communication. In this

paper, we formulated a throughput maximization problem under multiple sets of constraints to cater to a cognitive radio based I-SAT network. To efficiently solve the optimization problem, the formulated non-convex problem is divided into three subproblems, namely user association, transmission power optimization, and UAV trajectory control, by using the block descent method. The solution for each subproblem is thoroughly investigated. Contingent on the solutions, the original problem is solved in an iterative way, providing a low-complexity joint multi-domain optimization technique. The proposed method uses a segment-by-segment approach, which divides the entire UAV flight trajectory into smaller time segments to reduce calculation time. Finally, extensive numerical results were presented to demonstrate the enhanced throughput performance of the proposed scheme in comparison to different benchmark techniques.

REFERENCES

[1] Y. Liang, J. Tan, H. Jia, J. Zhang, and L. Zhao, "Realizing intelligent spectrum management for integrated satellite and terrestrial networks," *J. Commun. Inf. Netw.*, vol. 6, no. 1, pp. 32–43, 2021.

[2] H. Abou-Zeid, F. Pervez, A. Adinoyi, M. Aljlayl, and H. Yanikomeroglu, "Cellular V2X transmission for connected and autonomous vehicles standardization, applications, and enabling technologies," *IEEE Consum. Electron. Mag.*, vol. 8, no. 6, pp. 91–98, Nov. 2019.

[3] J. Navarro-Ortiz, P. Romero-Diaz, S. Sendra, P. Ameigeiras, J. J. Ramos-Munoz, and J. M. Lopez-Soler, "A survey on 5G usage scenarios and traffic models," *IEEE Commun. Surveys Tuts.*, vol. 22, no. 2, pp. 905–929, 2nd Quart., 2020.

[4] F. Pervez, C. Yang, and L. Zhao, "Dynamic resource management to enhance video streaming experience in a C-V2X network," in *Proc. IEEE 92nd Veh. Technol. Conf.*, Victoria, BC, Canada, Nov. 2020, pp. 1–5.

[5] S. Cioni, R. De Gaudenzi, O. D. R. Herrero, and N. Girault, "On the satellite role in the era of 5G massive machine type communications," *IEEE Netw.*, vol. 32, no. 5, pp. 54–61, Sep. 2018.

[6] S. Fu, J. Gao, and L. Zhao, "Collaborative multi-resource allocation in terrestrial-satellite network towards 6G," *IEEE Trans. Wireless Commun.*, early access, May 21, 2021, doi: 10.1109/TWC.2021.3080578.

[7] P. Naseri, S. A. Matos, J. R. Costa, C. A. Fernandes, and N. J. G. Fonseca, "Dual-band dual-linear-to-circular polarization converter in transmission mode application to *K/Ka*-band satellite communications," *IEEE Trans. Antennas Propag.*, vol. 66, no. 12, pp. 7128–7137, Dec. 2018.

[8] L. Wang, H. Yang, J. Long, K. Wu, and J. Chen, "Enabling ultra-dense UAV-aided network with overlapped spectrum sharing: Potential and approaches," *IEEE Netw.*, vol. 32, no. 5, pp. 85–91, Sep./Oct. 2018.

[9] L. Zhang and Y.-C. Liang, "Joint spectrum sensing and packet error rate optimization in cognitive IoT," *IEEE Internet Things J.*, vol. 6, no. 5, pp. 7816–7827, Oct. 2019.

[10] F. Pervez, L. Zhao, and C. Yang, "Intelligent cognition in an integrated satellite-aerial-terrestrial network for connected vehicles," in *Proc. Biennial Symp. Commun. (BSC)*, Saskatoon, SK, Canada, 2021.

[11] A. J. Roumeliotis, C. I. Kourogiorgas, and A. D. Panagopoulos, "Optimal dynamic capacity allocation for high throughput satellite communications systems," *IEEE Wireless Commun. Lett.*, vol. 8, no. 2, pp. 596–599, Apr. 2019.

[12] H. T. Nguyen, H. D. Tuan, T. Q. Duong, H. V. Poor, and W.-J. Hwang, "Joint D2D assignment, bandwidth and power allocation in cognitive UAV-enabled networks," *IEEE Trans. Cognit. Commun. Netw.*, vol. 6, no. 3, pp. 1084–1095, Sep. 2020.

[13] M. M. Azari, F. Rosas, A. Chiumento, and S. Pollin, "Coexistence of terrestrial and aerial users in cellular networks," in *Proc. IEEE Globecom Workshops*, Singapore, Dec. 2017, pp. 1–6.

[14] H. Wang, G. Ren, J. Chen, G. Ding, and Y. Yang, "Unmanned aerial vehicle-aided communications: Joint transmit power and trajectory optimization," *IEEE Wireless Commun. Lett.*, vol. 7, no. 4, pp. 522–525, Aug. 2018.

[15] W. Mei and R. Zhang, "Uplink cooperative NOMA for cellular-connected UAV," *IEEE J. Sel. Areas Commun.*, vol. 13, no. 3, pp. 644–656, Jun. 2019.

[16] S. Fu, Y. Tang, N. Zhang, L. Zhao, S. Wu, and X. Jian, "Joint unmanned aerial vehicle (UAV) deployment and power control for Internet of Things networks," *IEEE Trans. Veh. Technol.*, vol. 69, no. 4, pp. 4367–4378, Apr. 2020.

[17] Y. E. Sagduyu, Y. Shi, A. B. MacKenzie, and Y. T. Hou, "Regret minimization for primary/secondary access to satellite resources with cognitive interference," *IEEE Trans. Wireless Commun.*, vol. 17, no. 5, pp. 3512–3523, May 2018.

[18] Y. Ruan, Y. Li, C.-X. Wang, R. Zhang, and H. Zhang, "Power allocation in cognitive satellite-vehicular networks from energy-spectral efficiency tradeoff perspective," *IEEE Trans. Cogn. Commun. Netw.*, vol. 5, no. 2, pp. 318–329, Jun. 2019.

[19] Z. Li, F. Xiao, S. Wang, T. Pei, and J. Li, "Achievable rate maximization for cognitive hybrid satellite-terrestrial networks with AF-relays," *IEEE J. Sel. Areas Commun.*, vol. 36, no. 2, pp. 304–313, Feb. 2018.

[20] S. Shi, G. Li, K. An, Z. Li, and G. Zheng, "Optimal power control for real-time applications in cognitive satellite terrestrial networks," *IEEE Commun. Lett.*, vol. 21, no. 8, pp. 1815–1818, Aug. 2017.

[21] C. Liu, W. Feng, Y. Chen, C.-X. Wang, and N. Ge, "Cell-free satellite-UAV networks for 6G wide-area Internet of Things," *IEEE J. Sel. Areas Commun.*, vol. 39, no. 4, pp. 1116–1131, Apr. 2021.

[22] M. Li, N. Cheng, J. Gao, Y. Wang, L. Zhao, and X. Shen, "Energy-efficient UAV-assisted mobile edge computing: Resource allocation and trajectory optimization," *IEEE Trans. Veh. Technol.*, vol. 69, no. 3, pp. 3424–3438, Mar. 2020.

[23] J. Ji, K. Zhu, D. Niyato, and R. Wang, "Joint cache placement, flight trajectory, and transmission power optimization for multi-UAV assisted wireless networks," *IEEE Trans. Wireless Commun.*, vol. 19, no. 8, pp. 5389–5403, Aug. 2020.

[24] M. Najafi, H. Ajam, V. Jamali, P. D. Diamantoulakis, G. K. Karagiannidis, and R. Schober, "Statistical modeling of the FSO fronthaul channel for UAV-based communications," *IEEE Trans. Commun.*, vol. 68, no. 6, pp. 3720–3736, Jun. 2020.

[25] Y. Zeng, J. Xu, and R. Zhang, "Rotary-wing UAV enabled wireless network: Trajectory design and resource allocation," in *Proc. IEEE Global Commun. Conf.*, Abu Dhabi, UAE, Dec. 2018, pp. 1–6.

[26] J. Lyu, Y. Zeng, and R. Zhang, "UAV-aided offloading for cellular hotspot," *IEEE Trans. Wireless Commun.*, vol. 17, no. 6, pp. 3988–4001, Jun. 2018.

[27] Q. Wu, Y. Zeng, and R. Zhang, "Joint trajectory and communication design for multi-UAV enabled wireless networks," *IEEE Trans. Wireless Commun.*, vol. 17, no. 3, pp. 2109–2121, Mar. 2018.

[28] O. Abbasi, H. Yanikomeroglu, A. Ebrahimi, and N. M. Yamchi, "Trajectory design and power allocation for drone-assisted NR-V2X network with dynamic NOMA/OMA," *IEEE Trans. Wireless Commun.*, vol. 19, no. 11, pp. 7153–7168, Nov. 2020.

[29] K. Guo *et al.*, "Physical layer security for multiuser satellite communication systems with threshold-based scheduling scheme," *IEEE Trans. Veh. Technol.*, vol. 69, no. 5, pp. 5129–5141, May 2020.

[30] T. Zhou, Z. Liu, J. Zhao, C. Li, and L. Yang, "Joint user association and power control for load balancing in downlink heterogeneous cellular networks," *IEEE Trans. Veh. Technol.*, vol. 67, no. 3, pp. 2582–2593, Mar. 2018.

[31] S. Gopalam, S. V. Hanly, and P. Whiting, "Distributed user association and resource allocation algorithms for three tier HetNets," *IEEE Trans. Wireless Commun.*, vol. 19, no. 12, pp. 7913–7926, Dec. 2020.

[32] P. He, L. Zhao, S. Zhou, and Z. Niu, "Water-filling: A geometric approach and its application to solve generalized radio resource allocation problems," *IEEE Trans. Wireless Commun.*, vol. 12, no. 7, pp. 3637–3647, Jul. 2013.

[33] P. He, S. Zhang, L. Zhao, and X. Shen, "Energy-efficient power allocation with individual and sum power constraints," *IEEE Trans. Wireless Commun.*, vol. 17, no. 8, pp. 5353–5366, Aug. 2018.

[34] G. Interdonato, M. Karlsson, E. Bjornson, and E. G. Larsson, "Local partial zero-forcing precoding for cell-free massive MIMO," *IEEE Trans. Wireless Commun.*, vol. 19, no. 7, pp. 4758–4774, Jul. 2020.

[35] S. Boyd and L. Vandenberghe, *Convex Optimization*. Cambridge, U.K.: Cambridge Univ. Press, 2004.

[36] S. Yin, L. Li, and F. R. Yu, "Resource allocation and basestation placement in downlink cellular networks assisted by multiple wireless powered UAVs," *IEEE Trans. Veh. Technol.*, vol. 69, no. 2, pp. 2171–2184, Feb. 2020.

Farhan Pervez received the M.Sc. degree in communications engineering from the Technical University of Munich, Germany. He is currently pursuing the Ph.D. degree with the Department of Electrical, Computer, and Biomedical Engineering, Ryerson University, Toronto, Canada. He has several years of research experience in both academia and the communications industry. His research interests include wireless communications, integrated terrestrial and non-terrestrial networks, mobile edge computing, artificial intelligence, and optimization techniques.

Lian Zhao (Senior Member, IEEE) received the Ph.D. degree from the Department of Electrical and Computer Engineering, University of Waterloo, Canada. She is currently a Professor with the Department of Electrical, Computer, and Biomedical Engineering, Ryerson University, Toronto, Canada. Her research interests include wireless communications, resource management, mobile edge computing, caching and communications, and vehicular *ad-hoc* networks. She has been an IEEE Communication Society (ComSoc) Distinguished Lecturer (DL). She is a Licensed Professional Engineer at the Province of Ontario. She is a Senior Member of the IEEE Communication Society and the Vehicular Technology Society. She has severed as a panel expert for the Discovery Grant Program, and Evaluation Committee for the Research Tools and Instruments Grants Program of Natural Sciences Engineering Research Council of Canada (NSERC). She received the Best Land Transportation Paper Award from IEEE Vehicular Technology Society in 2016, the Top 15 Editor Award in 2016 for IEEE TRANSACTION ON VEHICULAR TECHNOLOGY, the Best Paper Award from the 2013 International Conference on Wireless Communications and Signal Processing (WCSP), and the Canada Foundation for Innovation (CFI) New Opportunity Research Award in 2005. She served as the Co-Chair of Wireless Communication Symposium for IEEE Globecom 2020 and IEEE ICC 2018; the Finance Co-Chair for 2021 ICASSP; the Local Arrangement Co-Chair for IEEE VTC Fall 2017 and IEEE Infocom 2014; the Co-Chair of Communication Theory Symposium for IEEE Globecom 2013. She has been serving as an Editor for IEEE TRANSACTIONS ON WIRELESS COMMUNICATIONS, IEEE INTERNET OF THINGS JOURNAL, and IEEE TRANSACTIONS ON VEHICULAR TECHNOLOGY.

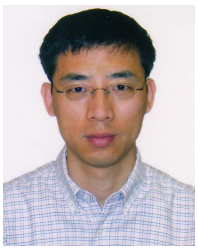

Cungang Yang received the Ph.D. degree in computer science from the University of Regina, Canada, in 2003. He is currently an Associate Professor with the Department of Electrical, Computer and Biomedical Engineering, Ryerson University. His research interests include cloud security, artificial intelligence in vehicles, the Internet of Things (IoT) security, wireless mesh networks, and role-based access control (RBAC).